JACS
JOURNAL OF THE AMERICAN CHEMICAL SOCIETY
Article
pubs.acs.org/JACS

Sorting of Lipidated Peptides in Fluid Bilayers: A Molecular-Level Investigation

Trevor A. Daly,[†] Paulo F. Almeida,*[,‡] and Steven L. Regen*[,†]

[†]Department of Chemistry, Lehigh University, Bethlehem, Pennsylvania 18105, United States

[‡]Department of Chemistry and Biochemistry, University of North Carolina Wilmington, Wilmington, North Carolina 28403, United States

Supporting Information

ABSTRACT: Nearest-neighbor recognition (NNR) measurements have been made for two lipidated forms of GlyCys, interacting with analogues of cholesterol and 1,2-dipalmitoyl-*sn*-glycero-3-phosphocholine (DPPC) in the liquid-ordered (l_o) and liquid-disordered (l_d) phases. Interaction free energies that have been determined from these measurements have been used in Monte Carlo simulations to quantify the distribution of the peptides between liquid-ordered and liquid-disordered regions. These simulations have shown that significant differences in the lipid chains have a very weak influence on the partitioning of the peptide between these two phases. They have also revealed an insensitivity of the peptide partition coefficient, K_p, to the size of the l_o and l_d domains that are present. In a broader context, these findings strongly suggest that the sorting of peripheral proteins in cellular membranes via differential lipidation may be more subtle than previously thought.

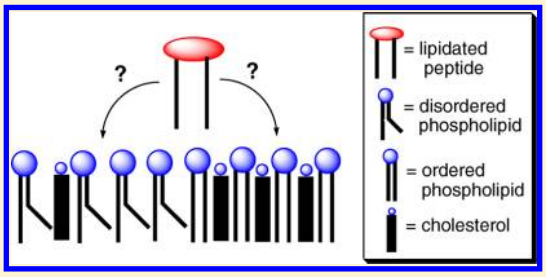

INTRODUCTION

One of the greatest challenges presently facing chemists, biochemists and biophysicists is to define the two-dimensional structure of cell membranes. In particular, the time-averaged lateral distribution of the lipids and proteins that make up these natural enclosures remains to be established. Over the past decade, a popular model for mammalian membranes has emerged that is based on the "lipid raft hypothesis."[1−7] Specifically, it has been proposed that cholesterol and high-melting sphingolipids form fluctuating nanoscale assemblies (lipid rafts) that float in a "sea" of low-melting lipids. It has also been postulated that lipid rafts serve as organizing media for peripheral proteins and that the nature of the lipids used to anchor these proteins to membranes controls their partitioning between raft and nonraft regions, a process that has been referred to as lipid sorting.[1] Thus, saturated hydrocarbon chains and sterols are thought to favor the association with lipid rafts while short, branched, and unsaturated hydrocarbon chains having one or more *cis*-double bonds (chains having permanent "kinks") are believed to favor partitioning into more fluid regions.[1,8]

Fluorescence spectroscopy and microscopy, atomic force microscopy, and surface plasmon resonance have been used to investigate sorting of lipidated proteins in ternary model membranes, such as mixtures of 1,2-dipalmitoyl-*sn*-glycero-3-phosphocholine (DPPC), 1,2-dioleoyl-*sn*-glycero-3-phosphocholine (DOPC), and cholesterol.[9−13] Ternary systems have proven especially popular because they produce macroscopic (μm-size) liquid-ordered (l_o) and liquid-disordered (l_d) domains that coexist and can be readily visualized.

We have begun a program that is aimed at gaining deeper insight into lipid sorting by placing it on a more quantitative basis. Our approach uses experimentally determined values of nearest-neighbor interaction free energies, ω_{AB}, in combination with Monte Carlo computer simulations.[14−16] Of particular significance is the fact that *this approach is applicable to domains of any size and that it can provide a detailed molecular-level view of membrane organization.*

Here we show how this strategy yields detailed molecular-level insight into the mixing behavior of two lipidated peptides (**1** and **2**, Chart 1) with analogues of cholesterol and DPPC (**3** and **4**, Chart 1) in host membranes of DPPC and cholesterol in the l_o/l_d coexistence region. This binary system was of special interest to us because its phase behavior has been well studied and because discrete microdomains are thought to be present in this coexistence region but have never actually been visually observed, a situation that is analogous to putative microdomains in cellular membranes.[17−19] The two lipidated peptides designed for this investigation are analogs of [(myristoyl)GlyCys(palmitoyl)-]. It has been suggested that this moiety represents a minimal sequence that is necessary for promoting efficient association with lipid rafts; for example, with the lck-EGFP chimera protein in COS-7 cells.[9] In one of our analogues, a permanent kink was introduced in its C14 chain to assess the consequences of coiling the lipid anchor on the mixing properties of the lipidated peptide.

Received: July 30, 2012

   dx.doi.org/10.1021/ja3074825 | J. Am. Chem. Soc. XXXX, XXX, XXX−XXX

EXPERIMENTAL METHODS

Nearest-Neighbor Recognition Measurements. Thin films of lipid were prepared by evaporating a chloroform solution containing 11.7 μmol total lipid (2.5 mol % of each exchangeable lipid, and 95 mol % DPPC/1,2-dipalmitoyl-*sn*-glycero-3-phosphoglycerol (DPPG)/Cholesterol). For the exact composition of the lipid mixtures used for all NNR reactions, see the Supporting Information. After drying the thin film overnight under reduced pressure (0.4 mmHg) at room temperature, 2.0 mL of a 10 mM Tris-HCl buffer (10 mM Tris, 150 mM NaCl, 2 mM NaN_3, 1 mM EDTA, pH = 7.4) was added to the dried film. The lipids were then dispersed by vortex mixing for 30 s, followed by incubation for 5 min at 60 °C, vortex mixing for an additional 30 s, and incubation for an additional 30 min at 60 °C with intermittent vortexing. The resulting dispersion was then subjected to six freeze/thaw cycles (liquid nitrogen/60 °C water bath) and extruded 20 times through a 200 nm pore diameter polycarbonate filter (Nuclepore, Whatman, Inc.) using argon at a pressure of ~100 psi. An 60 μL aliquot of 1.68 μM monensin in Tris-HCl buffer was then added to aid in pH equilibration across the membrane during NNR reactions.

The vesicle dispersion (1600 μL) was heated to 45 °C and oxygen was removed by purging with argon. A thiolate-disulfide interchange reaction was then initiated by adding *threo*-dithiothreitol (12.0 μL of a 25.1 mM solution in pH 7.4 Tris buffer, 1.0 equiv with respect to disulfide content) and sufficient amount of 0.1 M NaOH to bring the pH to 7.4 at 45 °C. Aliquots (250 μL) were withdrawn as a function of time, and the exchange reaction quenched by adding 25 μL of 8.3 M acetic acid to the test tube containing these aliquots, along with vortex mixing 10 s and quickly freezing the dispersion using liquid nitrogen. Aliquots were stored at −20 °C until analysis by HPLC was carried out. To each thawed aliquot was then added 1000 μL of $CHCl_3$/MeOH (2/1, v/v) and aldrithiol-2 (2,2′-dipyridyldisulfide, 30 μL of a 10 mM solution in $CHCl_3$), and the tube vortex mixed, centrifuged, and the aqueous phases removed using a Pasteur pipet. The organic phase was then concentrated under reduced pressure using a Savant SVC-100 SpeedVac concentrator equipped with a cold trap and vacuum pump (~1 h at ~0.4 Torr). The lipids were then dissolved in 20 μL of $CHCl_3$ and 80 μL of the HPLC mobile phase. These samples were then analyzed by HPLC using a C18 reversed phase column and a flow rate of 0.9 mL/min. The mobile phases were composed of 10 mM *n*-Bu_4NOAc in ethanol/water/hexane 76/13/10 (v/v/v) (mobile phase A) or 77.5/11/11 (v/v/v) (mobile phase B). (See the Supporting Information for the gradients used for each analysis.) The column was maintained at 31 °C and the components were monitored at 203 nm. Values of K ($K = [\mathbf{AB}]^2/([\mathbf{AA}] \times [\mathbf{BB}])$) were calculated from peak areas obtained from the HPLC chromatograms using appropriate calibration curves; values that are reported are mean values after dimer equilibrium was reached, typically, within 12 h.

Differential Scanning Calorimetry. Suspensions of lipidated peptide samples (heterodimers {**1**−**4**} and {**2**−**4**} (Chart 1), and **2**′, the methyl sulfide derivative of **2**) were prepared by hydrating the lipid film at 85−95 °C in buffer, pH 7.5 (10 mM potassium phosphate or 20 mM MOPS, 0.1 mM EGTA, 0.02% NaN_3, and 100 mM KCl). Concentrations were estimated by weight and (for phosphate-containing dimers, {**1**−**4**} and {**2**−**4**}) by a modified Bartlett phosphate method.[20] The heat capacity of the aqueous suspensions (degassed under vacuum of 500 mmHg for 10 min) was measured using a high sensitivity Nano DSC (TA Instruments, New Castle, DE), equipped with 300 μL twin gold capillary cells, under a slight pressure (set once to 3 atm). The scan rate was 0.1 °C/min. The DSC curves were corrected by baseline subtraction as previously described.[21]

Monte Carlo Simulations. Monte Carlo simulations were performed using the model and methods recently described for DPPC/cholesterol,[22] with standard Monte Carlo procedures.[23−25] The lipid membrane was represented by a triangular lattice, with skew-periodic boundary conditions, where each site is occupied by a phospholipid, a lipidated peptide, or a cholesterol molecule. Equilibrium configurations of the lattice were generated using two types of steps: a non-nearest-neighbor Kawasaki step,[26] in which lipids are exchanged by randomly selecting partners on the lattice, and a Glauber step,[27] in which the lipid is switched between gel, l_d and l_o states. Cholesterol is considered to have only one state. The choice between attempted moves is aleatory. Acceptance is based on the Metropolis criterion[28] with a move probability that depends exponentially on the free energy change,[22−24,28] using a random number for the decision.[29] The simulations were performed in 100 × 100 lattices, but it was previously shown that simulations in lattices of 200 × 200 and 300 × 300 sites yield equivalent results in this type of system.[22,30] A Monte Carlo cycle is defined as a number of attempted moves identical to the number of lattice sites. The calculations included a pre-equilibration period of 5×10^4 Monte Carlo cycles followed by a period of 10^6 acquisition cycles, which were more than sufficient to obtain equilibrium properties. One lipid−lipid interaction parameter (ω_{AB}) is used for each pair of possible states (gel, l_o and l_d) and lipid species (Chart 1, **1**, **2**, **3**, and **4**) present in the system, which is defined by[16]

$$\omega_{AB} = \varepsilon_{AB} - \frac{\varepsilon_{AA} + \varepsilon_{BB}}{2} \quad (1)$$

Here, ε_{AB} represents the contact (nearest-neighbor) interaction between lipids A and B, which can be any combination of species and states. In addition, the simulations use the experimental values of the enthalpy (ΔH) and the transition temperatures (T_m) of the main phase transition of the phospholipids and lipidated peptides to calculate the probabilities of changing the lipid state. The model of Almeida[22] was used for DPPC and its analogue, **4**. In this model, the phospholipid accesses essentially only the gel and the l_d states in the absence of cholesterol, but has one more accessible thermodynamic state, l_o, which is intermediate in enthalpy and entropy, in the presence of cholesterol. The enthalpy of the l_o state is assumed to lie at 40% of the way between those of the gel and l_d.[22] Because lipidated peptides **1** and **2** resemble phospholipids, having a polar headgroup and two hydrocarbon chains, we have assumed that they behave similarly to DPPC regarding gel-to-fluid phase transitions. The important feature of the model for its present use is to treat the existence of gel, l_o and l_d states for the phospholipids and for the presumed gel, l_o, and l_d states of the lipidated peptides in a simple way. The model parameters pertaining to **1** and **2**, however, have little effect on the phase behavior of DPPC/cholesterol, especially because the lipidated peptides only occur in small amounts in the mixtures studied. Except in the cases determined here experimentally by nearest-neighbor recognition measurements (Table 1), the ω_{AB} interaction parameters were the same as those previously used for DPPC/cholesterol,[20] Namely, for gel-l_o and l_d−l_o interactions ω_{AB} = +330 cal/mol, and for gel-l_d interactions ω_{AB} = +360 cal/mol, where A and B are any phospholipids (DPPC or **4**) or lipidated peptides (**1** or **2**). The complete set of parameters is listed in Table SI4 (Supporting Information). The T_m and ΔH values of the chain-melting transition for **1** and **2** were estimated from differential scanning calorimetry (DSC) experiments.

RESULTS AND DISCUSSION

The Nearest-Neighbor Recognition (NNR) Method. As discussed elsewhere, the nearest-neighbor recognition (NNR) method is a chemical technique that probes lipid mixing at the molecular level.[14,31] Thus, NNR measurements take molecular-level snapshots of bilayer organization by detecting and quantifying the thermodynamic tendency of exchangeable monomers to become nearest-neighbors of one another. Typically, two lipids of interest (**A** and **B**) are converted into exchangeable dimers (homodimers **AA** and **BB**, and heterodimer **AB**) via the introduction of disulfide bonds, which are then allowed to undergo monomer interchange via thiolate-disulfide exchange (Figure 1). The resulting equilibrium that is established is governed by an equilibrium constant, $K = [\mathbf{AB}]^2/([\mathbf{AA}][\mathbf{BB}])$. When lipid monomers **A** and **B** mix ideally, this is reflected by an equilibrium constant that equals 4.0; when homoassociations are favored, $K < 4.0$, and when hetero-

dx.doi.org/10.1021/ja3074825 | J. Am. Chem. Soc. XXXX, XXX, XXX−XXX

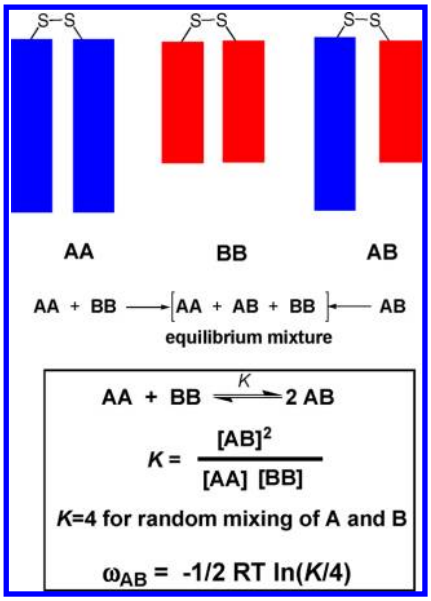

Figure 1. A stylized illustration showing the exchangeable homodimers, **AA** and **BB** and the corresponding heterodimer, **AB**, as well as the equations that describe the dimer equilibrium and the relationship between the equilibrium constant, K, and the corresponding nearest-neighbor interaction free energy, ω_{AB}, between **A** and **B**.

associations are favored $K > 4.0$. Taking statistical considerations into account, nearest-neighbor interaction free energies between **A** and **B** are then given by $\omega_{AB} = -1/2RT \ln(K/4)$.[16] Values of ω_{AB} are the primary information that is sought in all NNR measurements.

The Exchangeable Lipidated Peptides. The exchangeable lipids that were designed for this study are shown in Chart 1. Lipidated peptide **1** is a mimic of [(myristoyl)GlyCys-

Chart 1

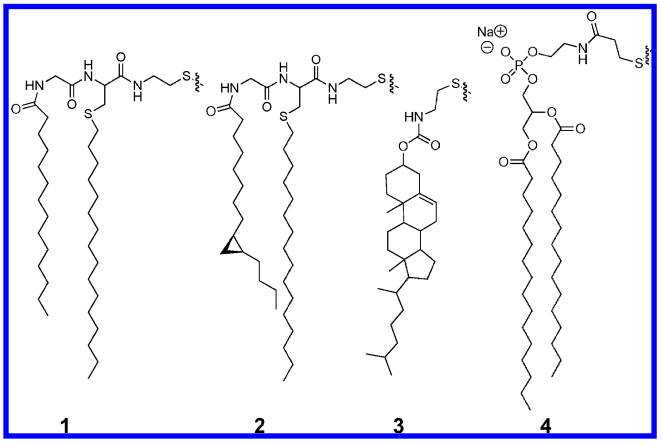

(palmitoyl)-], having the thioester carbonyl group replaced by a thioether linkage for enhanced stability. Lipidated peptide **2** is similar to **1**, except for a permanent kink in its C14 chain. Because double bonds undergo *cis*-/*trans*-isomerization under NNR conditions, a *cis*-cyclopropyl moiety was used to "lock in" a kink in **2**.[32] Exchangeable lipids **3** and **4** have previously been shown to be *excellent mimics for cholesterol and DPPC*, respectively, as judged by their membrane physical properties and their mutual mixing behavior.[33,34] Additionally, DPPC and **4**′, the methyl sulfide derivative of **4**, exhibit nearly identical gel-to-liquid crystalline phase transition temperatures, which are 41.5 and 39.9 °C, respectively.[34] We also note that **4** has an acidic head group, as DPPG, and because the mixing and physical properties of DPPC and DPPG are known to be similar, this exchangeable lipid can serve as a mimic for both phospholipids.

The synthetic method that was used to prepare the homodimer of **1** (i.e., {**1**–**1**}) is outlined in Scheme 1. Thus,

Scheme 1. Synthesis of {1–1}

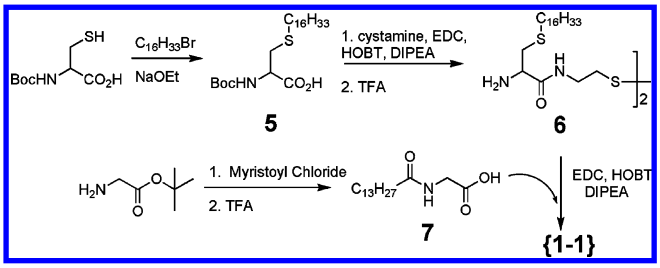

alkylation of Boc-protected cysteine with 1-bromohexadecane to give **5**, followed by condensation with cystamine and deprotection afforded **6**. Subsequent acylation with a myristoylated form of glycine (**7**) produced the requisite dimer, {**1**–**1**}. The corresponding heterodimer, composed of **1** and **3** (i.e., {**1**–**3**}), was prepared using a sequence of reactions shown in Scheme 2. Thus, activation of cholesterol with *N*,*N*′-

Scheme 2. Synthesis of {1–3}

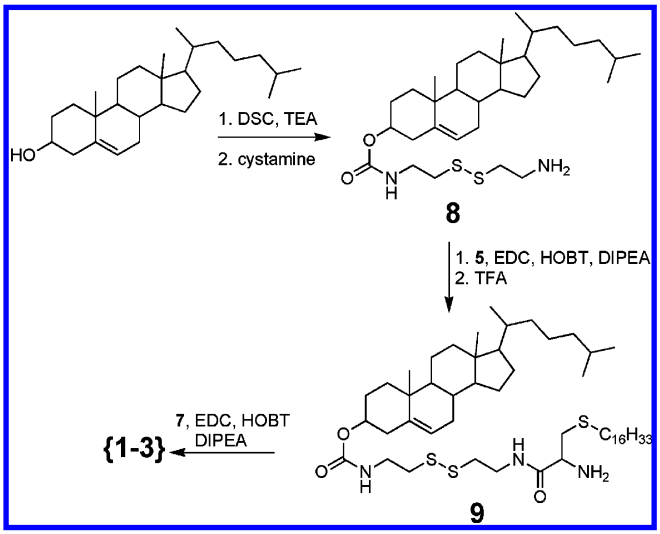

disuccinimidyl carbonate and condensation with cystamine afforded **8**, followed by condensation with **5**, deprotection and coupling to **7** afforded {**1**,**3**}. Heterodimer {**1**–**4**} was prepared by forming an activated derivative of 1,2-dipalmitoyl-*sn*-glycero-3-phosphoethanolamine (DPPE), **10**, followed by reaction with the thiol monomer of **1** (i.e., **1**-SH) (Scheme 3). The latter was obtained by reduction of {**1**–**1**} with tris(2-carboxyethyl)-phosphine (TCEP) (not shown). Related methods were used for the synthesis of homodimer {**2**–**2**} and the corresponding heterodimers, {**2**–**3**} and {**2**–**4**} (not shown), where myristic acid was replaced by the cylopropyl adduct of myristoleic acid (Supporting Informaton).

Nearest-Neighbor Interactions. For all of the NNR experiments that are reported herein, an equimolar mixture of

dx.doi.org/10.1021/ja3074825 | J. Am. Chem. Soc. XXXX, XXX, XXX–XXX

Scheme 3. Synthesis of {1−4}

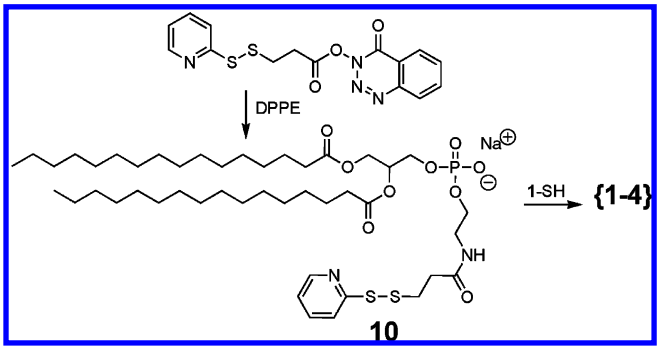

the exchangeable lipids (2.5 mol % of each lipid) was included in host membranes (95 mol %) that were made from a mixture of DPPC and cholesterol or only DPPC. For reactions using {**1**−**3**} or {**2**−**3**}, 2.5 mol % DPPG was included to give all liposomes used in these studies the same net negative charge. Cholesterol-rich and cholesterol-poor membranes were prepared with a total sterol content of 40 and 2.5 mol %, respectively. At the temperature used in this work (45 °C), the former is in the liquid-ordered (l_o) phase, and the latter is in the liquid-disordered (l_d), which are the phases that are commonly used as models for lipid rafts and more fluid regions of cell membranes.[35]

Using standard conditions that have been developed for carrying out thiolate-disulfide interchange in liposomal membranes, NNR measurements were made for the interactions of (i) **1** with **3** and **4**, and (ii) **2** with **3** and **4** in the l_o and l_d states. The interaction of **3** with **4** has previously been reported.[35] Our principal results are shown in Table 1.

Table 1. Nearest-Neighbor Recognition[a]

	l_o		l_d	
lipid pair	K	ω_{AB} (cal/mol)	K	ω_{AB}(cal/mol)
1,3	5.7 ± 0.4	−110 ± 23	2.8 ± 0.4	108 ± 41
1,4	4.0 ± 0.2	0.8 ± 14	4.8 ± 0.3	−55 ± 20
2,3	5.0 ± 0.3	−74 ± 21	2.7 ± 0.3	123 ± 31
2,4	8.0 ± 1.3	−219 ± 51	9.8 ± 0.6	−283 ± 19
3,4	9.8 ± 0.5	−282 ± 15	3.5 ± 0.1	40 ± 7

[a]All measurements were made at 45 °C.

In Figure 2 is shown an energy diagram that summarizes the interaction free energies, ω_{AB}, for each pair of lipids listed in Table 1. For ease of interpretation, they have been separated into three general categories: lipidated peptide-cholesterol (Pep-Chol), cholesterol-phospholipid (Chol-PL) and peptide-phospholipid (Pep-PL) interactions.

Inspection of this diagram reveals two distinct trends. First, the association of the cholesterol analogue (**3**) with both lipidated peptides (**1** and **2**) and with the phospholipid analogue (**4**) becomes *more* favorable on going from the l_d to the l_o phase. In particular, favored homoassociation in the l_d phase crosses over to favored heteroassociation in the l_o phase. In addition, this *change* is similar in magnitude in each case. Second, the association of each of the lipidated peptides (**1** and **2**) with the phospholipid analogue **4** becomes *less* favorable as one goes from the l_d to the l_o phase. Here also, the magnitude of these changes is similar in each case. Additionally, the difference between **1** and **2** associating with **4** is dramatic. Thus, whereas **1**

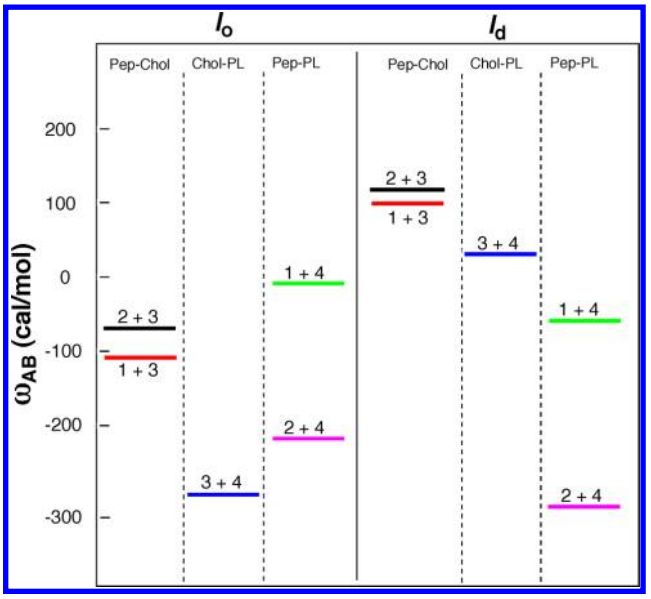

Figure 2. Energy diagram showing the nearest-neighbor interaction free energies, ω_{AB}, for various pair of lipids and lipidated peptides in the l_o phase (left) and the l_d phase (right), separated into peptide-cholesterol (Pep-Chol), cholesterol-phospholipid (Chol-PL) and peptide-phospholipid (Pep-PL) interactions.

and **4** mix randomly in the l_o phase and show a slight preference for heteroassociation in the l_d phase, **2** and **4** have a strong preference for heteroassociation in both phases. The fact that the *changes* that occur within each trend are similar in magnitude strongly suggests that they have a common origin.

We posit that these trends are best explained by (i) the well-known preference of cholesterol to associcate with ordered rather than "kinked" chains, (ii) a very unfavorable homointeraction between two molecules of **2** (kinked chains) in bilayers based on DPPC, and (iii) a tendency of lipid bilayers to maximize hydrocarbon chain packing. In considering these trends, it is important to keep in mind that *our experimental values of ω_{AB} do not represent absolute energies for the interactions between **A** and **B**. Rather, they are a measure of the difference in free energy between the heterointeractions and the average of the homointeractions* (eq 1).

First, let us consider the interactions between each of the lipidated peptides (**1** and **2**) and the phospholipid (**4**). In the case of **1** interacting with **4**, the mixing is, essentially, ideal in both the l_d and l_o phases. This finding implies that there are no special homo- or heterointeractions occurring in either phase. In contrast, there is a strong preference for heteroassociation between **2** and **4** in these same two phases. Since the headgroups of **1** and **2** are identical, this strong heteroassociation must be due to the "kink" that is present in **2**. Intuitively, one might suppose that some type of complex is being formed between **2** and **4** based on these large negative values of ω_{24}. However, the probability of complexation occurring in both the l_o and the l_d phases is very low. A much more plausible scenario is one in which favorable heteroassociation between **2** and **4** is driven by *unfavorable homointeractions* between two molecules of **2**. Thus, the poor packing efficiency of **2**, resulting from the presence of a "kink," leads to a homodimer, {**2**−**2**}, that is much less stable than the corresponding heterodimer, {**2**−**4**}. The heteroassociation between **2** and **4** becomes more favorable in the l_d phase because their packing behavior becomes better tolerated in a disordered state.[16]

dx.doi.org/10.1021/ja3074825 | J. Am. Chem. Soc. XXXX, XXX, XXX−XXX

Now let us consider the lipidated peptide-sterol and phospholipid-sterol interactions. Within experimental error, the interactions of the lipidated peptides (**1** and **2**) with the sterol (**3**) are identical in both the l_o and l_d phases (Table 1). Also, these heteroassociations are slightly less favorable (by ~100 cal/mol) than that found for **3** interacting with **4** (cholesterol and DPPC analogues). Whereas the mixing of **3** with **4** is close to ideal (i.e., $\omega_{34} \approx 0$) in the l_d phase, homoassociations are favored for **1** and **2** interacting with **3** in this same phase. The latter is a likely consequence of poor interactions between the rigid sterol and the disordered hydrocarbon chains of the lipidated peptides, which are spaced further apart than in the phospholipid. If the interactions between two molecules of **2** are, in fact, very unfavorable, then the association between **2** and **3** is also expected to be weak. This can account for the positive ω_{23}. It should be noted, in this regard, that unfavorable interactions between disordered (kinked) phospholipid chains and cholesterol are quite common.[16]

In the l_o phase, the net heteroassociation between **3** and **1**, **2**, and **4** (i.e., ω_{13}, ω_{23} and ω_{34}, respectively) is enhanced. At present, we believe this is mainly due to more favorable interactions between the sterol and the hydrocarbon chains that are now more ordered. Although unfavorable sterol−sterol interactions (ε) in the l_o phase can also account for more favorable heteroassociations (eq 1), we think that such contributions are likely to be of minor importance since only **1**, **2** and **4**, are capable of undergoing significant conformational changes between the l_d to the l_o phase; the conformation of the rigid sterol is, essentially, constant. The similarity in behavior among **1**, **2** and **4** that we have observed in these studies strongly suggests that these lipidated peptides access conformational states that are similar to those of DPPC, for which **4** is an analogue. However, the smaller negative values of ω_{13} and ω_{23}, relative to ω_{34}, indicate that the association between these lipidated peptides and the sterol are not quite as favorable as phospholipid−sterol association. In the Supporting Information section, we present a more quantitative analysis of these energy differences, which supports the conclusion that *nearest-neighbor interactions between two molecules of* **2**, *and also between a molecule of* **2** *interacting with a molecule of* **3**, *are especially weak*.

Chain Melting of the Lipidated Peptides. Both of the exchangeable lipidated peptides, **1** and **2**, bear a resemblance to common phospholipids by having one polar headgroup and two hydrocarbon chains. One might expect, therefore, that these peptides would exhibit similar gel to liquid-crystalline phase transition behavior. In an effort to explore this possibility, we first synthesized nonexchangeable derivatives of **1** and **2** (**1′** and **2′**, respectively), where the thiol moiety was "capped" with a methyl group (not shown). Attempted dispersal of **1′** in buffer proved impossible, even at temperatures as high as 80 °C. In contrast, **2′** could be dispersed at 80 °C. Examination of the latter by high-sensitivity DSC showed a well-defined endotherm with an apparent T_m of 61 °C. Because of the difficulty in quantifying the amount of **2′** present in this dispersion, a reliable enthalpy value could not be obtained.

In an alternative approach for gaining insight into the melting behavior of **1** and **2**, we examined the thermal properties of dispersions made from heterodimers {**1**−**4**} and {**2**−**4**}. Previously, we showed that the melting of exchangeable homodimers formed from **4**, as well as analogues bearing myristoyl and stearoyl chains (**4a** and **4b**, Chart 2) occurs at T_m that are nearly identical to those of phosphocholines with the same acyl chains.[34] We have also shown that the corresponding dimers exhibit enthalpies (ΔH) that are essentially additive of those of the monomers, and that the T_m values tend to be weighted more heavily in favor of the lower-melting lipid.[34] This bias toward the lower-melting lipid is analogous to what is known for phospholipids bearing two different acyl chains. For example, the T_m values for 1-palmitoyl-2-oleyol-*sn*-glycero-3-phosphocholine (POPC), 1,2-dioleyol-*sn*-glycero-3-phosphocholine (DOPC), and DPPC are −3, −18, and 41.5 °C, respectively.[36] This behavior is probably a consequence of disordering of the longer hydrocarbon chains by the lower-melting partner in the bilayer phase. On the basis of the data in Table 2, we can estimate ΔH and T_m for the chain melting of **1** and **2** from phospholipid-based heterodimers; that is, by assuming that ΔH for {**1**−**4**} and {**2**−**4**} are simply the sum of the corresponding monomers and, to a first approximation, that $T_m = (0.65 \times T_m^{low}) + (0.35 \times T_m^{high})$, where T_m^{low} and T_m^{high}

Chart 2

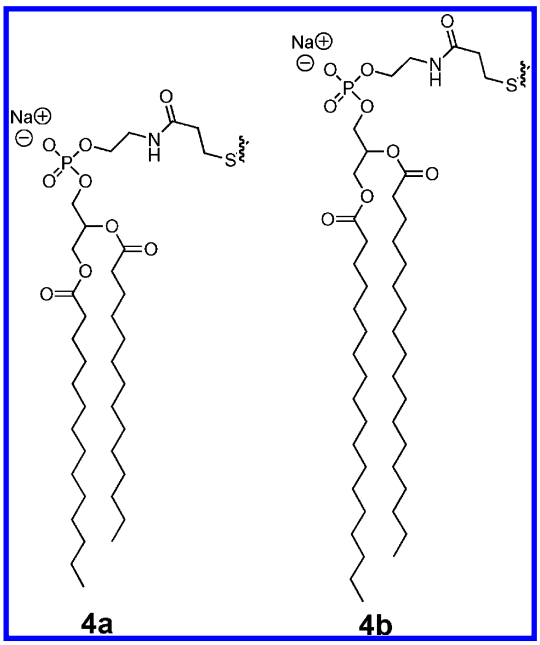

Table 2. Melting Behavior of Dimers and Monomers

	T_m (°C)		ΔH (kcal/mol)	
lipid	dimer	monomer[a]	dimer	monomer[a]
DMPC		23.8		6.1
{**4a**−**4a**}[b]	22.7		14.7	
DPPC		41.5		8.5
{**4**−**4**}[b]	41.9	39.9[c]	18.7	9.3[c]
DSPC		54.8		10.9
{**4b**−**4b**}[b]	55.4		21.7	
{**4a**−**4**}	−31.2	23.8, 41.5	16.7	~7[d], 10[d]
{**4a**−**4b**}[b]	33.9	23.8, 54.8	18.7	~7[d], 11[d]
{**1**−**4**}	55	~80[d], 41.5	~24	~10[d], 10[d]
{**2**−**4**}	45	61[e], 41.5	~17	~7[d], 10[d]

[a]The values given are for phosphocholines, 1,2-myristoyl-*sn*-glycero-3-phosphocholine (DMPC), DPPC, and 1,2-stearoyl-*sn*-glycero-3-phosphocholine (DSPC), and are from a combination of references (i.e., 36−44). [b]Taken from reference 34. [c]Value of **4′**. [d]Estimated value. [e]Value of **2′**.

dx.doi.org/10.1021/ja3074825 | J. Am. Chem. Soc. XXXX, XXX, XXX−XXX

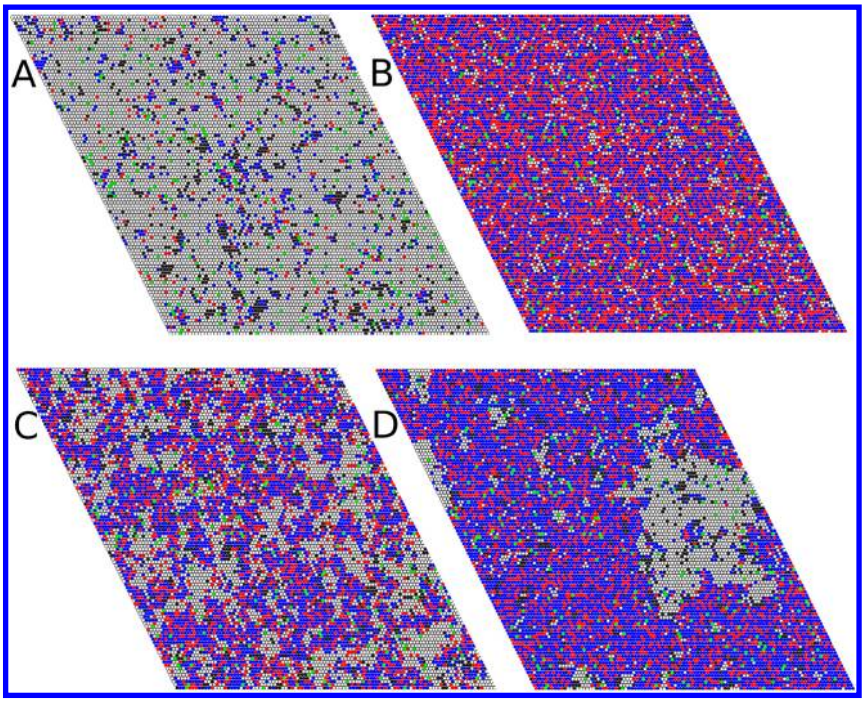

Figure 3. Snapshots of Monte Carlo simulations of mixtures of DPPC and cholesterol containing 2.5 mol % of **1**: (A) l_d phase, DPPC/cholesterol/**1**, 95/2.5/2.5 (mol/mol/mol); (B) l_o phase, DPPC/cholesterol/**1**, 57.5/40/2.5 (mol/mol/mol); (C) l_d/l_o coexistence region, DPPC/cholesterol/**1**, 77.5/20/2.5 (mol/mol/mol); (D) same as panel C, except that ω_{34} (nearest-neighbor interaction free energy between **3** and **4** in the l_d phase) has been artificially set at 400 cal/mol instead of the observed value of 40 cal/mol. DPPC is shown in black (gel), white (l_d), or blue (l_o); cholesterol is shown in red; and **1** is shown in green. No distinction is made between DPPC and **4**, and between cholesterol and **3**..

are the T_m values for the low and high-melting monomers (see Supporting Information for details).

Examination of {**1**−**4**} by DSC revealed a main transition at 55 °C with an apparent $\Delta H \approx 24 \pm 4$ kcal/mol. Given the monomer chains involved (similar to DPPC), this seems a little too large, and a value close to the lower bound, ∼20 kcal/mol, seems more reasonable. On the basis of these considerations, ΔH for **1** is estimated to be ∼10 kcal/mol. Further, using the approximation above, with $T_m = 55$ °C and $T_m^{low} = 41.5$ °C, we obtain $T_m^{high} \sim 80$ °C for **1**. Note that this high T_m value readily explains our inability to disperse **1**′. In contrast, {**2**−**4**} gave a broad and complex transition that was centered around 45 °C, with a significant dependence on the hydration temperature and thermal history (Supporting Information). Our best estimate for its overall enthalpy change is 17 ± 4 kcal/mol, which leads to an estimated ΔH of ∼7 kcal/mol for **2**, assuming that there is again a ∼10 kcal/mol contribution from the **4** moiety. It should be noted that the level of uncertainty affecting ΔH has a negligible effect on the Monte Carlo simulation results.[30] We consider the T_m of 61 °C, which we measured directly for **2**′, to be a more reliable estimate for the T_m of **2** than what could be calculated from the transition of the heterodimer {**2**−**4**}. We did not investigate the melting behavior of {**2**−**4**} further. Judging from the DSC, the phase transitions of all the heterodimers containing lipidated peptides are certainly more complex than a gel to fluid transition. However, all that is required for this study is an estimate of the tendency of monomers **1** and **2** to be in an ordered or disordered state, which is provided by T_m and, to a lesser extent, by ΔH. This is all the information we extract from the DSC results.

Monte Carlo Simulations. Lipid membranes were simulated as 100 × 100 triangular lattices, where each site represents a phospholipid, a lipidated peptide, or a sterol molecule. The phospholipids can exist in three states: gel, l_o, and l_d state. The l_o state is intermediate to the gel and l_d states in terms of its enthalpy, entropy, and chain order. Simulations were performed at the same temperature (45 °C) using NNR values that were now experimentally determined in each phase, in addition to those previously used for DPPC/cholesterol.[22] Snapshots of the simulations are shown in Figure 3 for the l_o, l_d, and l_o/l_d (20 mol % cholesterol) coexistence phases. DPPC is shown in black (gel), white (l_d), or blue (l_o); cholesterol is shown in red, and **1** is shown in green. No distinction is made between DPPC and **4**, or between cholesterol and **3**.

A partition coefficient for each lipidated peptide, **1** or **2**, was defined by their distribution between l_o and l_d regions of the membrane according to eq 2. Here, [**1** or **2**]$_o$ and [**1** or **2**]$_d$ represent the number of lipidated peptides in the l_o and l_d regions, and [l_o] and [l_d] are the number of phospholipid sites belonging to each region.

$$K_p = \frac{[\mathbf{1} \text{ or } \mathbf{2}]_o/[l_o]}{[\mathbf{1} \text{ or } \mathbf{2}]_d/[l_d]} \quad (2)$$

For these calculations, a lipidated peptide molecule was considered to be located in an l_o or l_d region according to the majority of nearest neighbor lipids surrounding it. In defining K_p, only phospholipid molecules were counted; the sites occupied by sterol were not counted for either phase. The results obtained for **1** and **2** in the l_d/l_o coexistence region (20 mol % cholesterol) are summarized in Table 3.

Because of the presence of long saturated hydrocarbon chains in **1**, we expected that this lipidated peptide would favor the l_o phase. This, however, did not prove to be the case. Rather, the peptide was evenly distributed between both phases ($K_p = 1.0$). In contrast, the presence of a permanent kink in **2**

dx.doi.org/10.1021/ja3074825 | J. Am. Chem. Soc. XXXX, XXX, XXX−XXX

Table 3. Partition Coefficients for 1 and 2[a]

lipid	phase behavior	ω_{34}[b] (cal/mol)	K_p (l_o/l_d)
1	small domains	40	1.0 ± 0.15
1	phase separation	400	1.2 ± 0.2
2	small domains	40	0.46 ± 0.07
2	phase separation	400	0.46 ± 0.07

[a]Determined from Monte Carlo simulations in membranes of DPPC/cholesterol/(1 or 2) 77.5/20/2.5 (mol/mol/mol). No distinction is made between DPPC and 4, and between cholesterol and 3. [b]The nearest-neighbor interaction free energy between 3 and 4 in the l_d phase was set either at the experimentally determined value of 40 cal/mol or at a hypothetical value of 400 cal/mol to strongly favor phase separation.

led to an expected preference for the l_d phase, albeit only modest ($K_p \approx 0.5$). To test if K_p actually depended on domain size, we carried out additional Monte Carlo simulations in which the nearest-neighbor interaction free energy between DPPC and cholesterol (ω_{34}) in the l_d phase was changed from the experimental value of 40 cal/mol to an artificial value of 400 cal/mol. As expected, this led to a system approaching true phase separation (Figure 3D). However, the calculated K_p in this artificial situation was essentially unchanged (Table 3). Thus, *the lack of a significant preference for these lipidated peptides to reside in either phase appears to be a robust property.*

Partitioning of other lipidated forms of GlyCys between a l_o and l_d phase have previously been investigated by Silvius and co-workers in host membranes made from DPPC, 1,2-dioleoyl-*sn*-glycero-3-phosphocholine and cholesterol using a fluorescence quenching assay.[9] In that study, it was shown that the introduction of a single *cis*-double bond in a myristoyl chain was sufficient to increase the peptide preference for the l_d phase. Qualitatively, our results are in complete agreement with those earlier findings.

Interpretation of Partition Coefficients. The partition coefficients, K_p, which characterize the partitioning of **1** and **2** between liquid-ordered and liquid-disordered regions, can be understood in a very simple way in terms of our nearest-neighbor interaction free energies. First, we can relate K_p to the change in interactions experienced by the lipidated peptides as they are transferred from the l_d to the l_o phase. Let us define a mean-field, $\Delta\omega$, for each lipidated peptide, **1** and **2**, which measures the change in the interactions upon transfer from the l_d to the l_o regions by a weighted average of the interactions in each region. Here, f_c^o and f_c^d are the mole fractions of cholesterol in the ordered and disordered regions, respectively, (the superscripts o and d indicate those two phases in eqs 3 and 4).

$$\Delta\omega_1 = (\omega_{13}^o f_c^o + \omega_{14}^o(1 - f_c^o)) - (\omega_{13}^d f_c^d + \omega_{14}^d(1 - f_c^d)) \quad (3)$$

$$\Delta\omega_2 = (\omega_{23}^o f_c^o + \omega_{24}^o(1 - f_c^o)) - (\omega_{23}^d f_c^d + \omega_{24}^d(1 - f_c^d)) \quad (4)$$

According to the mean-field approximation, the partition coefficient is then related to $\Delta\omega$ by

$$K_p = e^{-6\Delta\omega/RT} \quad (5)$$

where there are 6 nearest-neighbors in a triangular lattice. Using the values of K_p of 1.0 for **1** and 0.46 for **2**, we obtain $\Delta\omega_1 = 0$ for **1** and $\Delta\omega_2$= +80 cal/mol for **2** at 45 °C. Using these two values along with the interaction free energy values for ω_{13}, ω_{14}, ω_{23}, and ω_{24} in the two phases (determined by NNR measurements) in eqs 3 and 4, the mole fractions of cholesterol in the l_o and l_d regions are calculated to be $f_c^o = 0.36$ and $f_c^d = 0.08$. In other words, the cholesterol content in the l_o and l_d phases are estimated to be 36 and 8 mol %, respectively, which are very reasonable values given an overall cholesterol content of 20 mol % in this mixture and the phase diagram for DPPC/cholesterol.[22]

It should also be noted that this treatment then allows one to calculate K_p directly from the interaction parameters, ω_{AB}, if the cholesterol content in the two phases is known even if a true phase coexistence does not actually exist in the l_o/l_d region, but only small domains are present. This further illustrates the power of NNR measurements for probing lipid sorting at the molecular level. In summary, the values of K_p that we have calculated from these Monte Carlo simulations can be understood very simply and directly in terms of the experimental values of ω_{AB}. If they appear small, it is because the preference of the lipidated peptides between the l_d and l_o regions is, indeed, very weak.

CONCLUSIONS

In this paper, we have shown that nearest-neighbor recognition measurements, in combination with Monte Carlo simulations, afford reasonable estimates of the partition coefficients of lipidated peptides between liquid-ordered and liquid-disordered regions of fluid membranes. We have also shown that these partition coefficients are insensitive to the size of l_o and l_d domains. Our results further indicate that the NNR method, in combination with a phase diagram, should provide a good estimate of partitioning of a species between two phases.

In a broader context, the very weak directing effect that lipidation of GlyCys has on its partitioning between l_o and l_d regions, observed here, strongly suggests that the sorting of lipidated peripheral proteins on the basis of their fatty acyl chain modifications is more subtle than previously realized. Our results are reminiscent of those reported for the dual-lipidated peripheral protein N-Ras. With one farnesyl and one hexadecyl chain, N-Ras partitions to the l_d phase or to l_d–l_o interfaces, but not to the l_o phase.[11,12] This behavior is similar to that of our lipidated peptide **2**, which also contains a Cys-linked, ordered, hexadecyl chain and a kinked chain. Further, our lipidated peptide **1**, bearing one myristoyl and one hexadecyl chain, shows no preference for the l_o phase. In fact, even with two hexadecyl chains, N-Ras still prefers the l_d phase.[11] In other words, this peptide and protein, bearing long hydrocarbon chains that can exist in an all-anti conformation, show no special affinity to the l_o phase. .

Finally, from a biological standpoint, it should be noted that our results with these simple model systems are in complete agreement with a recent study of the dynamic colocalization of lipid-anchored fluorescent proteins in live COS 7 cells, using pulsed-interleaved excitation fluorescence cross-correlation spectroscopy (PIE-FCCS) and fluorescent lifetime analysis.[45] Specifically, neither study supports the view that the organization of lipidated proteins is determined, alone, by the partitioning of their lipid anchors between two lipid phases.

ASSOCIATED CONTENT

Supporting Information

Complete experimental procedures for the synthesis of the exchangeable lipids and for NNR measurements as well as raw

dx.doi.org/10.1021/ja3074825 | J. Am. Chem. Soc. XXXX, XXX, XXX–XXX

NNR data, DSC data, and a quantitative interpretation of the NNR results. This material is available free of charge via the Internet at http://pubs.acs.org.

AUTHOR INFORMATION

Corresponding Author

slr0@lehigh.edu; almeidap@uncw.edu

Notes

The authors declare no competing financial interest.

ACKNOWLEDGMENTS

We are grateful to our colleagues, Drs. Serhan Turkyilmaz, Ravil Petrov and Vaclav Janout for helpful discussions. This work was funded by the National Science Foundation (CHE-1145500), the National Institutes of Health (PHS GM56149) and North Carolina Biotechnology Center grant 2009-IDG-1031.

REFERENCES

(1) Lingwood, D.; Simons, K. *Science* **2010**, *327*, 46−50.

(2) McIntosh, T. J., Ed. *Lipid Rafts*; Springer Verlag: New York, NY, 2007.

(3) (a) Lichtenberg, D.; Goni, F. M.; Heerklotz, H. *Trends Biochem. Sci.* **2005**, *30*, 430−436. (b) Heerklotz, H. *Biophys. J.* **2002**, *83*, 2693−2701.

(4) Edidin, M. *Annu. Rev. Biomol. Struct.* **2003**, *32*, 257−283.

(5) Munro, S. *Cell* **2003**, *115*, 377−388.

(6) McMullen, T. P. W.; Lewis, R. N. A. H.; McElhaney, R. N. *Curr. Opin. Colloid Interface Sci.* **2004**, *8*, 459−468.

(7) Veatch, S.; Cicuta, P.; Sengupta, P.; Honerkamp-Smith, A; Holowka, D.; Baird, B. *ACS Chem. Biol.* **2008**, *3*, 287−293.

(8) Levental, I.; Grzybek, M.; Simons, K. *Biochemistry* **2010**, *49*, 6305−6316.

(9) Wang, T.-Y.; Leventis, R.; Silvius, J. R. *Biochemistry* **2001**, *40*, 13031−13040.

(10) Janosch, S.; Nicolini, C.; Ludloph, B.; Peters, C.; Voklert, M.; Hazlet, T. L.; Gratton, E.; Waldmann; Winter, R. *J. Am. Chem. Soc.* **2004**, *126*, 7496−7503.

(11) Weise, K.; Triola, G.; Brunsveld, L.; Waldmann, H.; Winter, R. *J. Am. Chem. Soc.* **2009**, *131*, 1557−1564.

(12) Weise, K.; Triola, G.; Janosch, S.; Waldmann, H.; Winter, R. *Biochim. Biophys. Acta* **2010**, *1798*, 1409−1417.

(13) Gohlke, A.; Triola, G.; Waldmann, H.; Winter, R. *Biophys. J.* **2010**, *98*, 2226−2235. Weise, K.; Kapoor, S.; Denter, C.; Nikolaus, J.; Opitz, N.; Koch, S.; Triola, G.; Herrmann, A.; Waldmann, H.; Winter, R. *J. Am. Chem. Soc.* **2011**, *133*, 880−887.

(14) (a) Davidson, S. K. M.; Regen, S. L. *Chem. Rev.* **1997**, *97*, 1269−1279. (b) Regen, S. L. *Curr. Opin. Chem. Biol.* **2002**, *6*, 720−735. (c) Cao, H.; Tokutake, N.; Regen, S. L. *J. Am. Chem. Soc.* **2003**, *125*, 16182−16183. (d) Sugahara, M.; Uragami, M.; Yan, X.; Regen, S. L. *J. Am. Chem. Soc.* **2001**, *123*, 7939−7940. (e) Mitomo, H.; Chen, W.-H.; Regen, S. L. *J. Am. Chem. Soc.* **2009**, *131*, 12354−12357. (f) Cao, H.; Zhang, J.; Jing, B.; Regen, S. L. *J. Am. Chem. Soc.* **2005**, *127*, 8813−8816. (g) Zhang, J.; Jing, B.; Tokutake, N.; Regen, S. L. *Biochemistry* **2005**, *44*, 3598−3603.

(15) Frazier, M. L.; Wright, J. R.; Pokorny, A.; Almeida, P. F. F. *Biophys. J.* **2007**, *92*, 2422−2433.

(16) Almeida, P. F. F. *Biochim. Biophys. Acta* **2009**, *1788*, 72−85.

(17) Recktenwald, D. J.; McConnell, H. M. *Biochemistry* **1981**, *20*, 4505−4510.

(18) Subramaniam, S.; McConnell, H. M. *J. Phys. Chem.* **1987**, *91*, 1715−1718.

(19) Collins, M. D.; Keller, S. L. *Proc. Natl. Acad. Sci. U.S.A.* **2008**, *105*, 124−128.

(20) Bartlett, G. R. *J. Biol. Chem.* **1959**, *234*, 466−468. Pokorny, A.; Birkbeck, T. H.; Almeida, P. F. F. *Biochemistry* **2002**, *41*, 11044−11056.

(21) Pokorny, A.; Yandek, L. E.; Elegbede, A. I.; Hinderliter, A.; Almeida, P. F. F. *Biophys. J.* **2006**, *91*, 2184−2197.

(22) Almeida, P. F. *Biophys. J.* **2011**, *100*, 420−429.

(23) Heimburg, T. *Thermal Biophysics of Membranes*; Wiley-VCH: Weinheim, Germany, 2007; pp 123−140.

(24) Sugar, I. P.; Biltonen, R. L.; Mitchard, N. *Methods Enzymol.* **1994**, *240*, 569−593.

(25) Binder, K.; Heerman, D. W. *Monte Carlo Simulations in Statistical Physics*, 3rd ed.; Springer: New York, 1997.

(26) Kawasaki, K. Kinetics of Ising Models. In *Phase Transitions and Critical Phenomena*; Domb, C., Green, M. S., Eds.; Academic Press: New York, 1972; Vol. 2, pp 443−501.

(27) Glauber, R. J. *J. Math. Phys.* **1963**, *4*, 294−307.

(28) Metropolis, N.; Rosenbluth, A. W.; Rosenbluth, W. N.; Teller, A. H.; Teller, E. *J. Chem. Phys.* **1953**, *21*, 1087−1092.

(29) Press, W. H.; Teukolsky, S. A.; Vetterling, W. T.; Flannery, B. P. *Numerical Recipes in FORTRAN: The Art of Scientific Computing*, 2nd ed.; Cambridge University Press: Cambridge U.K., 1994.

(30) Svetlovics, J. A.; Wheaten, S. A.; Almeida, P. F. *Biophys. J.* **2012**, *102*, 2526−2535.

(31) In contrast to other methods that have been used to determine ω_{AB} values (i.e., differential scanning calorimetry, fluorescence resonance energy transfer, isothermal titration calorimetry, and analyses of phase diagrams), the NNR method does not require any matching of experimental data with theoretical curves.[16] It is also highly sensitive and can detect changes in free energies of interaction down to tens of calories per mole.

(32) Jing, B.; Tokutake, N.; McCullough, D. H., III; Regen, S. L. *J. Am. Chem. Soc.* **2004**, *126*, 15344−15345.

(33) Zhang, J.; Cao, H.; Jing, B.; Almeida, P. F.; Regen, S. L. *Biophys. J.* **2006**, *91*, 1402−1406.

(34) Kristovitch, S. M.; Regen, S. L. *J. Am. Chem. Soc.* **1992**, *114*, 9828−9835.

(35) Daly, T. A.; Wang, M.; Regen, S. L. *Langmuir* **2011**, *27*, 2159−2161.

(36) *Phospholipids Handbook*; Cevc., G., Ed.; Marcel Dekker: New York, 2001; pp 939−956.

(37) Hac, A. E.; Seeger, H. M.; Fidorra, M.; Heimburg, T. *Biophys. J.* **2005**, *88*, 317−333.

(38) Ivanova, V. P.; Heimburg, T. *Phys. Rev. E.* **2001**, *63*, 1914−1925.

(39) Suurkuusk, J.; Lentz, B. R.; Barenholz, Y.; Biltonen, R. L.; Thompson, T. E. *Biochemistry* **1976**, *15*, 1393−1401.

(40) Mabrey, S.; Sturtevant, J. *Proc. Natl. Acad. Sci. U.S.A.* **1976**, *73*, 3862−3866.

(41) Estep, T. N.; Mountcastle, D. B.; Biltonen, R. L.; Thompson, T. E. *Biochemistry* **1978**, *17*, 1984−1989.

(42) Blume, A. *Biochemistry* **1983**, *22*, 5436−5442.

(43) Marsh, D. *CRC Handbook of Phospholipid Bilayers*; CRC Press: Boca Raton, FL, 1990; p 149.

(44) Koyonova, R.; Caffrey, M. *Biochim. Biophys. Acta* **1998**, *1376*, 91−145.

(45) Triffo, S. B.; Huang, H. H.; Smith, A. W.; Chou, E. T.; Groves, J. T. *J. Am. Chem. Soc.* **2012**, *134*, 10833−10842.